Available online at www.sciencedirect.com
SCIENCE DIRECT®
Journal of Sound and Vibration 286 (2005) 529–547
JOURNAL OF SOUND AND VIBRATION
www.elsevier.com/locate/jsvi

A Volterra series approximation to the coherence of the Duffing oscillator

K. Worden*, G. Manson

Dynamics Research Group, Department of Mechanical Engineering, University of Sheffield, Mappin Street, Sheffield S1 3JD, UK

Received 13 November 2003; received in revised form 7 October 2004; accepted 12 October 2004
Available online 1 January 2005

Abstract

Following previous work on computing approximate frequency response functions for the Duffing oscillator under white Gaussian excitation, an approximation is obtained here for the coherence function. A Padé approximation of order (1,1) is made for the asymmetric Duffing oscillator (i.e. with non-zero quadratic term), and an approximation of order (2,2) is made for the symmetric (no quadratic term) oscillator. The analytical results are shown to give excellent qualitative agreement with numerical simulation. However, in quantitative terms, the approximations underpredict the coherence distortion as is consistent with the low-order truncations of the Volterra series.

1. Introduction

This paper forms the latest in a series which attempts to form analytical approximations to structural dynamic observables using the Volterra functional series. In the first two [1,2], approximations to the nonlinear composite frequency response function (FRF) were obtained for a symmetric and asymmetric Duffing oscillator and a two degree-of-freedom (dof) system with a cubic stiffness nonlinearity, respectively. The approximations, which were obtained for the specific case of white Gaussian excitation, reproduced the correct qualitative behaviour of the FRFs as

*Corresponding author. Tel.: +44 114 222 7758; fax: +44 114 222 7890.
E-mail address: k.worden@sheffield.ac.uk (K. Worden).

0022-460X/$ - see front matter © 2004 Elsevier Ltd. All rights reserved.
doi:10.1016/j.jsv.2004.10.028

Nomenclature

FRF	frequency response function
HFRF	higher-order FRF
sdof	single degree-of-freedom
$E[]$	expectation operator
$H(\omega)$	linear FRF
$H_n(\omega_1,\ldots,\omega_n)$	nth-order Volterra kernel transform
P	power-spectral density
$S_{uu}(\omega)$	auto-power spectrum of $u(t)$
$S_{uv}(\omega)$	cross-power spectrum between $u(t)$ and $v(t)$
$h(t)$	linear impulse response
$h_n(t_1,\ldots,t_n)$	nth-order Volterra kernel
k_2, k_3	quadratic and cubic stiffness parameters
m, c, k	linear system parameters (mass, damping, stiffness)
t, τ	time
t'	normalised time
$x(t)$	excitation
$y(t)$	displacement response of system
$y_n(t)$	nth-order component of response
$\Lambda_r(\omega)$	composite FRF of nonlinear system
γ	coherence
$\gamma_{(i,j)}$	(i,j)-order Padé approximation to the coherence
$\delta(\omega)$	Dirac delta function
$\phi_{uu}(\tau)$	auto-correlation function of $u(t)$
$\phi_{uv}(\tau)$	cross-correlation function between $u(t)$ and $v(t)$
ω	circular frequency
ω_d	damped natural frequency
ω_n	undamped natural frequency
ζ	damping ratio

Superscript stars denote complex conjugation.

the level of excitation increased, i.e. in the single-dof (sdof) case, the 'resonance' peak in the FRF shifted upwards in frequency and downwards in amplitude as the level of forcing increased. The motivation for the calculations is the need to understand if the Volterra series is applicable to structural dynamics at realistic levels of forcing. That the levels of excitation applied in Refs. [1,2] are realistic follows from the fact that the frequency shifts observed from the calculations are consistent with those seen in experiments.

Another interesting feature of the calculations was the suggestion that all the FRF poles, including poles generated at multiples of the linear system poles, were in the upper half of the complex plane. This contrasts directly with low-order approximations for the FRF under sinusoidal excitation and goes some way to explaining why the Hilbert transform test for nonlinear systems fails for random excitation, yet works well for stepped-sine forcing.

The current paper extends the previous calculations by computing an approximation to the coherence for the asymmetric and symmetric Duffing oscillators. Unlike the previous calculations that were polynomial in P, the power of the white Gaussian excitation, the new calculation is necessarily a rational or Padé approximation and thus a little more complicated. It could be argued that the calculations have only academic interest, given the uncertainty which surrounds the application of the Volterra series. However, as the levels of excitation used here produce frequency shifts which are consistent with experiment and the convergence of the series is established at these levels [1], the authors feel that the analysis does make contact with reality. The authors also feel that analytical results always contribute some insight and there is the possibility of using the functional forms obtained by the route shown here for nonlinear system identification if the excitation is appropriately low (but also high enough to excite the nonlinearity of course).

The layout of the paper is as follows. Section 2 reviews the necessary background on the Volterra series in general, and in the particular case of the sdof Duffing oscillator. Section 3 discusses how the Padé approximations are formed from the various cross-spectra involved. Sections 4 and 5 construct the approximations in the asymmetric and symmetric cases of the Duffing oscillator, respectively. The paper concludes with some discussion in Section 6.

2. FRFs and cross-spectra

The coherence for a linear system is constructed as the ratio of certain cross-spectra and auto-spectra, or alternatively in terms of the FRF and the auto-spectra. Before proceeding to the construction of the coherence function for a nonlinear system in terms of a Volterra series expansion, it is useful to recall the definitions of the FRFs and cross-spectra for such systems in terms of the Volterra series.

It is well-known that many nonlinear systems or input–output processes $x(t) \longrightarrow y(t)$ can be realised as a mapping [3,4],

$$y(t) = y_1(t) + y_2(t) + y_3(t) + \cdots + y_n(t) + \cdots, \tag{1}$$

where

$$y_n(t) = \int_{-\infty}^{+\infty} \cdots \int_{-\infty}^{+\infty} \mathrm{d}\tau_1 \ldots \mathrm{d}\tau_n \, h_n(\tau_1, \ldots, \tau_n) x(t-\tau_1) \ldots x(t-\tau_n). \tag{2}$$

Among the conditions for such a series to apply are time-invariance of the system of interest and polynomial nature for the nonlinearity.

This is the *Volterra series* and the functions h_n are the *Volterra kernels*. The dual frequency-domain representation is based on the *higher-order FRFs* (HFRFs) or *Volterra kernel transforms*, $H_n(\omega_1, \ldots, \omega_n)$, $n = 1, \ldots, \infty$, which are defined as the multi-dimensional Fourier transforms of the kernels.

$$H_n(\omega_1, \ldots, \omega_n) = \int_{-\infty}^{+\infty} \cdots \int_{-\infty}^{+\infty} \mathrm{d}\tau_1 \ldots \mathrm{d}\tau_n \, h_n(\tau_1, \ldots, \tau_n) \mathrm{e}^{-\mathrm{i}(\omega_1\tau_1 + \cdots + \omega_n\tau_n)}. \tag{3}$$

The definition of the FRF of a linear system based on the input/output cross-spectrum, $S_{yx}(\omega)$, and input autospectrum, $S_{xx}(\omega)$, is also well-known,

$$H(\omega) = H_1(\omega) = \frac{S_{yx}(\omega)}{S_{xx}(\omega)}, \tag{4}$$

where the spectral quantities are defined as expectations i.e. $S_{yx}(\omega) = E[\overline{Y}(\omega)X(\omega)]$. The expectations are obtained by averaging discrete or fast Fourier transforms from neighbouring time segments.

The *composite FRF* $\Lambda_r(\omega)$, of a nonlinear system under random excitation, is defined similarly,

$$\Lambda_r(\omega) = \frac{S_{yx}(\omega)}{S_{xx}(\omega)}. \tag{5}$$

Using the Volterra series representation in (1) results in the expression

$$\Lambda_r(\omega) = \frac{S_{y_1x}(\omega) + S_{y_2x}(\omega) + \cdots + S_{y_nx}(\omega) + \cdots}{S_{xx}(\omega)}. \tag{6}$$

$\Lambda_r(\omega)$ was approximated in Ref. [1] by obtaining expressions for the various cross-spectra between the input and the individual output components. The general term used was

$$S_{y_{2n-1}x}(\omega) = \frac{(2n)!S_{xx}(\omega)}{n!2^n(2\pi)^{n-1}} \int_{-\infty}^{+\infty} \cdots \int_{-\infty}^{+\infty} \mathrm{d}\omega_1 \ldots \mathrm{d}\omega_{n-1} \times H_{2n-1}(\omega_1, -\omega_1, \ldots, \omega_{n-1}, -\omega_{n-1}, \omega) S_{xx}(\omega_1) \ldots S_{xx}(\omega_{n-1}). \tag{7}$$

Now, given that the input autospectrum is constant over all frequencies for a white noise input (i.e. $S_{xx}(\omega) = P$), the composite FRF for random excitation follows. Substituting the constant S_{xx} into (7) gives

$$\Lambda_r(\omega) = \sum_{n=1}^{n=\infty} \frac{(2n)!P^{n-1}}{n!2^n(2\pi)^{n-1}} \times \int_{-\infty}^{+\infty} \cdots \int_{-\infty}^{+\infty} \mathrm{d}\omega_1 \ldots \mathrm{d}\omega_{n-1}\, H_{2n-1}(\omega_1, -\omega_1, \ldots, \omega_{n-1}, -\omega_{n-1}, \omega). \tag{8}$$

The system of interest here is going to be the basic asymmetrical Duffing oscillator with equation of motion,

$$m\ddot{y} + c\dot{y} + ky + k_2y^2 + k_3y^3 = x(t), \tag{9}$$

where m is the mass and c is the damping constant. k, k_2 and k_3 are the linear, quadratic and cubic stiffnesses, respectively. This system is time-invariant as required for the application of the Volterra series.

Note that this system can be unstable at high levels of excitation in the cases where $k_3 \leqslant 0$. In the analysis here where $k_3 \neq 0$ it is always positive and this ensures stability. For the case when k_3 is set to zero, the excitation level used here is not high enough to induce instability. Setting k_3 to zero here is purely a device to simplify the analysis, in practice it would be assumed that the asymmetric oscillator always has a higher-order odd term to ensure stability.

The relevant higher-order FRFs of this system for the forthcoming analysis are

$$H_1(\omega) = \frac{1}{-m\omega^2 + \mathrm{i}c\omega + k}, \tag{10}$$

$$H_2(\omega_1, \omega_2) = -k_2H_1(\omega_1)H_1(\omega_2)H_1(\omega_1 + \omega_2), \tag{11}$$

$$H_3(\omega_1, \omega_2, \omega_3) = H_1(\omega_1)H_1(\omega_2)H_1(\omega_3)H_1(\omega_1 + \omega_2 + \omega_3) \times \left\{ \frac{2}{3} k_2^2(H_1(\omega_1 + \omega_2) + H_1(\omega_2 + \omega_3) + H_1(\omega_3 + \omega_1)) - k_3 \right\} \tag{12}$$

for the asymmetric case when ($k_2 \neq 0$), and

$$\begin{aligned} H_5(\omega_1,\omega_2,\omega_3,\omega_4,\omega_5) &= \frac{3}{10}k_3^2 H_1(\omega_1+\omega_2+\omega_3+\omega_4+\omega_5)H_1(\omega_1)H_1(\omega_2)H_1(\omega_3)H_1(\omega_4)H_1(\omega_5) \\ &\times\{H_1(\omega_1+\omega_2+\omega_3)+H_1(\omega_1+\omega_2+\omega_4)+H_1(\omega_1+\omega_2+\omega_5) \\ &+ H_1(\omega_1+\omega_3+\omega_4)+H_1(\omega_1+\omega_3+\omega_5) \\ &+ H_1(\omega_1+\omega_4+\omega_5)+H_1(\omega_2+\omega_3+\omega_4)+H_1(\omega_2+\omega_3+\omega_5) \\ &+ H_1(\omega_2+\omega_4+\omega_5)+H_1(\omega_3+\omega_4+\omega_5)\} \end{aligned} \tag{13}$$

for the situation with $k_2 = 0$.

The assumption throughout is that the appropriate auto- and cross-spectra are well-defined. In fact, the theoretical white noise signal applied here is not physical as it has infinite variance (power). This does not matter in practice as any measured signal will always have finite power. The assumption of whiteness does not invalidate the analysis as it is largely valid as long as the real bandwidth of the input signal is wide enough to cover the natural frequency of the sdof system and any significant superharmonics [5].

3. Padé approximations for the coherence

The well-known expression for the coherence of a linear system is

$$\gamma^2(\omega) = \frac{S_{yx}(\omega)S_{xy}(\omega)}{S_{xx}(\omega)S_{yy}(\omega)} = \frac{|H(\omega)|^2 S_{xx}(\omega)}{S_{yy}(\omega)}, \tag{14}$$

where the interpretation is that the coherence is the ratio of the power in the output *linearly correlated with the measured input* divided by the power in the output. For a linear system, one expects this ratio to be unity. It is a textbook calculation [6], to show that the coherence is always less than unity if measurement noise is present on the input or output. It is also well-known that the coherence falls below unity if the system in question is nonlinear, although this belief is considerably less well-supported theoretically.

It is worth noting that the coherence is not infallible and it is possible to observe erroneous high coherence [7]. However, it can only occur in the case where multiple inputs to the system are present—which is not the case here. Even in the case of multiple correlated inputs, progress is possible by computing the partial coherences, however this is not pursued here.

Assuming that the coherence is computed from the auto and cross-spectra as in the linear case, the expression in the nonlinear case is simply

$$\gamma^2(\omega) = \frac{S_{yx}(\omega)S_{xy}(\omega)}{S_{xx}(\omega)S_{yy}(\omega)} = \frac{|\Lambda_r(\omega)|^2 S_{xx}(\omega)}{S_{yy}(\omega)} \tag{15}$$

with reference to Eq. (14). In terms of the individual Volterra components of the signal y, this becomes,

$$\gamma^2(\omega) = \frac{(S_{y_1x}(\omega) + S_{y_3x}(\omega) + S_{y_5x}(\omega) + \cdots)(S_{xy_1}(\omega) + S_{xy_3}(\omega) + S_{xy_5}(\omega) + \cdots)}{S_{xx}(\omega)(S_{y_1y_1}(\omega) + S_{y_1y_3}(\omega) + S_{y_3y_1}(\omega) + S_{y_2y_2} + \cdots)} \tag{16}$$

and this expression takes into account the fact that terms of the form $S_{y_nx}(\omega)$ can be shown to vanish identically when n is even as do terms $S_{y_my_n}(\omega)$ where $m+n$ is odd.

In terms of the dependence on the input level P, (with a slight abuse of notation) this looks like,

$$\gamma^2(\omega) = \frac{(\mathrm{O}(P) + \mathrm{O}(P^2) + \mathrm{O}(P^3) + \cdots)(\mathrm{O}(P) + \mathrm{O}(P^2) + \mathrm{O}(P^3) + \cdots)}{P(\mathrm{O}(P) + \mathrm{O}(P^2) + \mathrm{O}(P^2) + \mathrm{O}(P^3) + \cdots)} \tag{17}$$

so both the numerator and denominator are expanded in powers of P. This means that an approximation to the coherence will have the general Padé form

$$\gamma^2_{(m,n)} = \frac{\sum_{i=0}^{m} a_i P^i}{\sum_{i=0}^{n} b_i P^i}, \tag{18}$$

where m and n are the orders of approximation of the numerator and denominator, respectively. For the purposes of this paper we will take $m = n$.

To order (0,0), the expression for the coherence is

$$\gamma^2_{(0,0)}(\omega) = \frac{S_{y_1x}(\omega)S_{xy_1}(\omega)}{PS_{y_1y_1}(\omega)} = \frac{PS_{y_1y_1}(\omega)}{PS_{y_1y_1}(\omega)} = 1 \tag{19}$$

on using the first lemma of Appendix A. This shows that to this order the coherence is unaffected by the nonlinearity. To order (1,1), one obtains from Eq. (18) (suppressing the argument ω)

$$\gamma^2_{(1,1)} = \frac{S_{y_1x}S_{xy_1} + S_{y_1x}S_{xy_3} + S_{y_3x}S_{xy_1}}{P(S_{y_1y_1} + S_{y_1y_3} + S_{y_3y_1} + S_{y_2y_2})} = \frac{S_{y_1x}S_{xy_1} + 2\,Re\,S_{y_1x}S_{xy_3}}{P(S_{y_1y_1} + 2\,Re\,S_{y_1y_3} + S_{y_2y_2})} \tag{20}$$

and using the first lemma, from Appendix A, this becomes

$$\gamma^2_{(1,1)} = \frac{S_{y_1x}S_{xy_1} + 2\,Re\,S_{y_1x}S_{xy_3}}{S_{y_1x}S_{xy_1} + 2\,Re\,S_{y_1x}S_{xy_3} + PS_{y_2y_2}} = \frac{A_{11}}{A_{11} + B_{11}}, \tag{21}$$

where

$$A_{11} = S_{y_1x}S_{xy_1} + 2\,Re\,S_{y_1x}S_{xy_3} \tag{22}$$

and

$$B_{11} = PS_{y_2y_2}. \tag{23}$$

One can immediately observe that if the Duffing oscillator is symmetric and $k_2 = 0$, then $y_2 = 0$, $S_{y_2y_2} = B_{11} = 0$ and the expression for the coherence to this order collapses to $\gamma^2_{(1,1)} = 1$. So for the symmetric system, the coherence is still insensitive to the nonlinearity to this order. If the oscillator is asymmetric, one would expect some distortion to occur and this is shown in the next section. In the symmetric case, higher-order approximations are required. The (2,2) Padé approximation will be considered next, but to simplify matters the symmetric case

will be assumed.

$$\gamma^2_{(2,2)} = \frac{S_{y_1x}S_{xy_1} + S_{y_3x}S_{xy_3} + 2\,Re\,S_{y_1x}S_{xy_3} + 2\,Re\,S_{y_1x}S_{xy_5}}{P(S_{y_1y_1} + S_{y_1y_3} + S_{y_3y_1} + S_{y_3y_3} + S_{y_1y_5} + S_{y_5y_1})}. \tag{24}$$

A little rearrangement using Lemma 1 from Appendix A gives

$$\gamma^2_{(2,2)} = \frac{|S_{y_1x}|^2 + |S_{y_3x}|^2 + 2\,Re\,S_{y_1x}S_{xy_3} + 2\,Re\,S_{y_1x}S_{xy_5}}{|S_{y_1x}|^2 + 2\,Re\,S_{y_1x}S_{xy_3} + 2\,Re\,S_{y_1x}S_{xy_5} + PS_{y_3y_3}} \tag{25}$$

and using (A.33), one obtains

$$\gamma^2_{(2,2)} = \frac{A_{22}}{A_{22} + B_{22}}, \tag{26}$$

where

$$A_{22} = |S_{y_1x}|^2 + |S_{y_3x}|^2 + 2\,Re\,S_{y_1x}S_{xy_3} + 2\,Re\,S_{y_1x}S_{xy_5} \tag{27}$$

and

$$B_{22} = \frac{6P^4}{(2\pi)^2}\int_{-\infty}^{\infty}\int_{-\infty}^{\infty} \mathrm{d}\omega_1\,\mathrm{d}\omega_2 |H_3(\omega_1, \omega_1, -\omega - \omega_1 - \omega_2)|^2. \tag{28}$$

This shows that to (2,2) order, the coherence for the symmetric Duffing oscillator finally shows some sensitivity to the nonlinearity.

In the next two sections, the preceding equations will be used to compute the (1,1) and (2,2) Padé approximations for the asymmetrical and symmetrical Duffing oscillators, respectively.

4. The asymmetric oscillator—an approximation of order (1,1)

This section computes the coherence $\gamma^2_{(1,1)}$ for the asymmetric Duffing oscillator, i.e. that given by Eq. (9). This amounts to calculating the terms A_{11} and B_{11} from Eqs. (22) and (23).

In order to obtain A_{11}, it is necessary to calculate the quantities S_{y_1x} and S_{y_3x} (note that these are the complex conjugates of S_{xy_1} and S_{xy_3}, respectively). The first is simple and is given in Ref. [1] as $PH_1(\omega)$. The second is also computed in Ref. [1], but only for the simpler $k_2 = 0$ case, a little more work is needed when $k_2 \neq 0$. First, from Ref. [1],

$$S_{y_3x}(\omega) = \frac{3P^2}{2\pi}\int_{-\infty}^{\infty} \mathrm{d}\omega_1\, H_3(\omega_1, -\omega_1, \omega) \tag{29}$$

and from Eq. (12) of this paper,

$$H_3(\omega_1, -\omega_1, \omega) = H_1(\omega)^2|H_1(\omega_1)|^2\left\{\frac{2}{3}k_2^2(H_1(0) + H_1(\omega + \omega_1) + H_1(\omega - \omega_1)) - k_3\right\}. \tag{30}$$

Now $H_1(0) = 1/k$, and the terms with $H_1(\omega + \omega_1)$ and $H_1(\omega - \omega_1)$ can be shown to give the same value when integrated as in (29). This gives

$$S_{y_3x}(\omega) = \frac{3P^2}{2\pi}\left(\frac{2}{3}\frac{k_2^2}{k} - k_3\right)H_1(\omega)^2 \int_{-\infty}^{\infty} \mathrm{d}\omega_1 \, |H_1(\omega_1)|^2 + \frac{2P^2k_2^2}{\pi}\int_{-\infty}^{\infty} \mathrm{d}\omega_1 \, |H_1(\omega_1)|^2 H_1(\omega - \omega_1). \tag{31}$$

The first integral is standard in structural dynamics [1]. The second is a little more complicated but is readily evaluated by using the calculus of residues. (The computations are rather intensive and have been carried out here with the help of *Mathematica*.) The final result is

$$S_{y_3x}(\omega) = \frac{3P^2}{2ck}\left(\frac{2}{3}\frac{k_2^2}{k} - k_3\right)H_1(\omega)^2 + 2P^2k_2^2 H_1(\omega)^2 I_1(\omega), \tag{32}$$

where,

$$I_1(\omega) = \frac{-(\omega - 4\mathrm{i}\omega_n\zeta)}{mck(\omega - 2\mathrm{i}\omega_n\zeta)(\omega - 2\omega_d - 2\mathrm{i}\omega_n\zeta)(\omega + 2\omega_d - 2\mathrm{i}\omega_n\zeta)}. \tag{33}$$

So, substituting into (22) gives,

$$A_{11} = P^2|H(\omega)|^2\left\{1 + \frac{3P}{ck}\left(\frac{2}{3}\frac{k_2^2}{k} - k_3\right)Re\, H_1(\omega) + 4Pk_2^2\, Re(H_1(\omega)I_1(\omega))\right\}. \tag{34}$$

In order to complete the approximation for the coherence, it is necessary to evaluate $B_{11} = PS_{y_2y_2}(\omega)$ (Eq. (21)). This involves essentially the same manipulations as used in Appendix A and in Ref. [1] so the detailed analysis will not be given here. The result in the general case is

$$B_{11} = \frac{P^3}{2\pi}\left\{\left(\int_{-\infty}^{\infty} \mathrm{d}\omega_1 \, H_2(\omega_1, -\omega_1)\right)^2 \delta(\omega) + 2\int_{-\infty}^{\infty} \mathrm{d}\omega_1 \, |H_2(\omega_1, \omega - \omega_1)|^2\right\}. \tag{35}$$

Using Eq. (11) for the asymmetric Duffing oscillator gives

$$B_{11} = \frac{P^3}{2\pi}\left\{\left(-\frac{k_2}{k}\int_{-\infty}^{\infty} \mathrm{d}\omega_1 \, |H_1(\omega_1)|^2\right)^2 \delta(\omega) + 2k_2^2|H_1(\omega)|^2 \int_{-\infty}^{\infty} \mathrm{d}\omega_1 \, |H_1(\omega_1)|^2 |H_1(\omega - \omega_1)|^2\right\}, \tag{36}$$

where $\delta(\omega)$ is the Dirac delta function. (Note that it is an abuse of notation to have this function appearing outside of an integral. It is used here to show that the first integral only affects the dc component of B_{11}.)

The first integral is the familiar standard, and the second is again obtained by using the calculus of residues. The result is

$$B_{11} = P^3k_2^2\left\{\frac{\pi}{2c^2k^4}\,\delta(\omega) + |H_1(\omega)|^2 I_2(\omega)\right\}, \tag{37}$$

where

$$I_2(\omega) = \frac{2(\omega^2 + 4\omega_d^2 + 20\omega_n^2\zeta^2)}{m^2ck(\omega^2 + 4\omega_n^2\zeta^2)([\omega + 2\omega_d]^2 + 4\omega_n^2\zeta^2)([\omega - 2\omega_d]^2 + 4\omega_n^2\zeta^2)}. \tag{38}$$

As A_{11} and B_{11} are now available, it is straightforward to compute the Padé (1,1) approximation to the coherence using Eq. (21). The formula was embedded in Fortran code and the approximations for the values $P = 0.005$, 0.01 and 0.02 were used as in Ref. [1] to generate Fig. 1 for $\gamma^2_{1,1}$. Unlike the situation in Ref. [1] for the symmetric Duffing oscillator, there is no readily available expression for the radius of convergence of the Volterra series in the asymmetric case so the convergence of the Volterra series for the higher values of P are not necessarily assured, A large effect is evident because of the high value of the k_2 coefficient—the values used for the simulation here were $m = 1$, $c = 20$, $k = 10^4$, $k_2 = 10^7$ and $k_3 = 5 \times 10^9$. These values give an undamped natural frequency ω_n of 100 rad/s and a damping ratio of 0.1 (10% of critical damping). With the parameters chosen, this figure shows excellent agreement with the coherence shown in Fig. 8 of Ref. [8]. This agreement is very encouraging as the figure in question represents the coherence for a simulated rotor with a breathing crack. The crack induces a bilinear nonlinearity which has a dominant even component which to a first approximation can be represented by the asymmetric Duffing oscillator. The slight distortion around the natural frequency for $P = 0.01$ is not evident in the simulation from Ref. [8] and probably arises from a higher relative contribution from k and k_3 in the current analysis.

The dips in the coherence occur when the ratio B_{11}/A_{11} is greatest. Clearly this will occur at the poles of B_{11} and the zeros of A_{11}. Leaving aside the latter quantities as they are not straightforward to obtain analytically, the poles of B_{11} occur in the vicinity of $\omega = 0$ and $\omega = 2\omega_d$ according to Eq. (38). This explains the main behaviour observed in Fig. 1.

In order to see what degree of FRF distortion this corresponds to, the $O(P)$ approximation to $\Lambda_r(\omega)$ is plotted in Fig. 2. This is

$$\Lambda_r(\omega) = H_1(\omega) + \frac{3P}{2ck}\left(\frac{2k_2^2}{3k} - k_3\right)H_1(\omega)^2 - 2Pk_2^2H_1(\omega)^2I_1(\omega), \tag{39}$$

where $I_1(\omega)$ is defined in Eq. (33). Although one cannot directly contrast the results from the (1,1) Padé approximation with the linear approximation to the FRF, one might venture that a small (3%) change in natural frequency here corresponds to a gross reduction in coherence.

In order to do a final validation, the equation of motion (9) was integrated numerically using a fourth-order Runga–Kutta scheme. The coefficient values were the same as in the Padé approximation described above. The excitation was a Gaussian white noise sequence with rms values chosen to correspond to the P values above. This in itself was not trivial as the Gaussian sequence was filtered into the interval [0,200] Hz in order to ensure correct behaviour of the Runga–Kutta routine. This lowered the rms from the required value and the final simulation used a corrected rms to account for this. 190 000 points of data for each case were taken and the coherence was estimated from a 512-line FFT, this gave 185 averages. The results are shown in comparison with the analytical results in Fig. 3. It is observed that

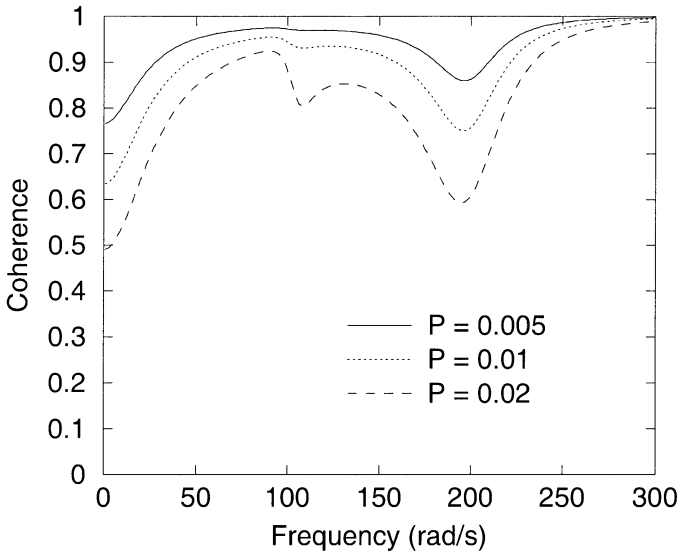

Fig. 1. Coherence from (1,1) Padé approximation for asymmetrical ($k_2 \neq 0$) Duffing oscillator: $P = 0.005$ (solid line), $P = 0.01$ (dotted), $P = 0.02$ (dashed).

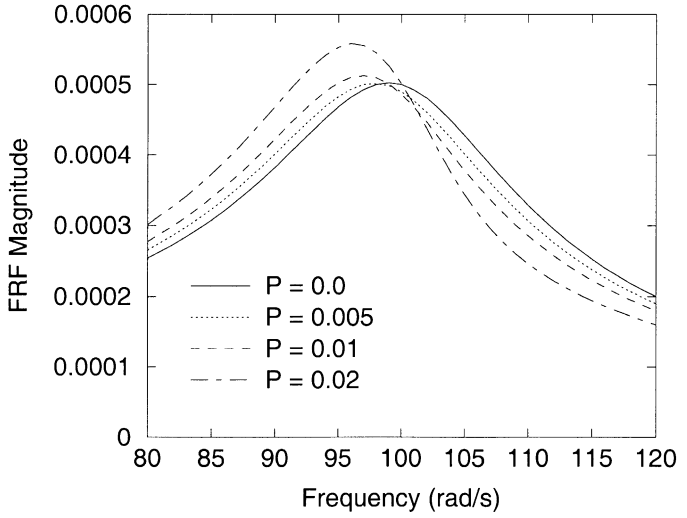

Fig. 2. FRF from O(P) approximation for asymmetrical ($k_2 \neq 0$) Duffing oscillator: $P = 0.0$ (solid line), $P = 0.005$ (dotted), $P = 0.01$ (dashed), $P = 0.02$ (dot-dash).

the best correspondence is for $P = 0.005$ as one might expect. Qualitatively the results are quite good, although the analytical results appear to underpredict the distortion. There is also an indication in the numerical results of a dip in coherence at three-times the natural frequency, which is consistent with excitation of the cubic term at higher values of P. This effect is not predicted at the $(1, 1)$ level of approximation.

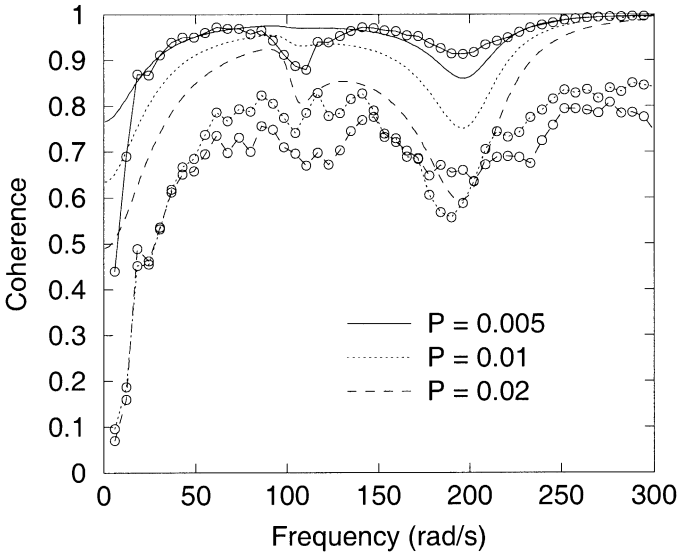

Fig. 3. Coherence from (1,1) Padé approximation for asymmetrical ($k_2 \neq 0$) Duffing oscillator: $P = 0.005$ (solid line), $P = 0.01$ (dotted), $P = 0.02$ (dashed). Comparison with numerical simulation (lines with circles).

5. The symmetric oscillator—an approximation of order (2,2)

This section computes the coherence $\gamma^2_{(2,2)}$ for the symmetric Duffing oscillator, i.e. that given by Eq. (9) with $k_2 = 0$. As described in Section 3, the coherence is insensitive to the nonlinearity at order (1,1) and this is why the higher-order approximation is necessary. This amounts to calculating the terms A_{22} and B_{22} from Eqs. (27) and (28). The necessary cross-spectra for A_{22} are from (27), S_{y_1x}, S_{y_3x} and S_{y_5x}. The first of these two quantities are given above (by setting $k_2 = 0$ for the asymmetric case), and the third was computed in Ref. [1]; it is

$$S_{y_5x}(\omega) = \frac{9}{2} P^3 k_3^2 H_1(\omega)^2 \left\{ \frac{1}{2c^2k^2} \left(H_1(\omega) + \frac{1}{k} \right) + I_3(\omega) \right\}, \tag{40}$$

where

$$I_3(\omega) = \frac{-(\omega^2 - 3\omega_d^2 - 10\mathrm{i}\omega_n\zeta\omega - 27\omega_n^2\zeta^2)}{mc^2k^2(\omega - \omega_d - 3\mathrm{i}\omega_n\zeta)(\omega + \omega_d - 3\mathrm{i}\omega_n\zeta)(\omega - 3\omega_d - 3\mathrm{i}\omega_n\zeta)(\omega + 3\omega_d - 3\mathrm{i}\omega_n\zeta)}. \tag{41}$$

The expression for the B_{22} term in Eq. (28), on using the expression (12) for H_3 with $k_2 = 0$, becomes,

$$B_{22}(\omega) = \frac{6k_3^2P^4}{4\pi^2} |H(\omega)|^2 \int_{-\infty}^{\infty} \mathrm{d}\omega_1 \, |H_1(\omega_1)|^2 \int_{-\infty}^{\infty} \mathrm{d}\omega_2 \, |H_1(\omega_2)|^2 |H_1(\omega - \omega_1 - \omega_2)|^2. \tag{42}$$

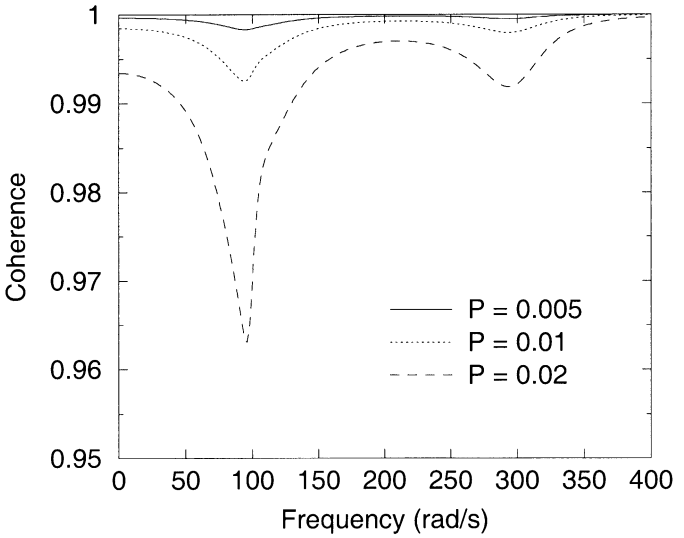

Fig. 4. Coherence from (2,2) Padé approximation for symmetrical ($k_2 = 0$) Duffing oscillator: $P = 0.005$ (solid line), $P = 0.01$ (dotted), $P = 0.02$ (dashed).

This is readily evaluated by contour integration (in fact the first integral has already been carried out for B_{11}). The result is

$$B_{22}(\omega) = \frac{9k_3^2P^4}{2m^2c^2k^2}|H(\omega)|^2 I_4(\omega), \tag{43}$$

where

$$I_4(\omega) = \frac{\omega^4 + 2\omega^2\omega_d^2 + 45\omega_d^4 + 54\omega^2\omega_n^2\zeta^2 + 522\omega_d^2\omega_n^2\zeta^2 + 1053\omega_n^4\zeta^4}{([\omega - \omega_d]^2 + 9\omega_n^2\zeta^2)([\omega + \omega_d]^2 + 9\omega_n^2\zeta^2)([\omega - 3\omega_d]^2 + 9\omega_n^2\zeta^2)([\omega + 3\omega_d]^2 + 9\omega_n^2\zeta^2)}. \tag{44}$$

The (2,2) Padé approximation to the coherence can now be computed using the expression in (26), the results for $P = 0.005$, 0.01 and 0.02 are shown in Fig. 4. The size of the distortion is small compared to the antisymmetric case. A comparison with numerical simulation is made in Fig. 5, the simulated data being generated in the same way as in the last section. It is seen that the Volterra approximation considerably underpredicts the coherence distortion, but is consistent with the fact that the $O(P^3)$ FRF prediction also underpredicts the frequency shift in the FRF [1]. The Padé approximation generates the correct features, i.e. is less than unity in the neighbourhood of the natural frequency and its third harmonic. However, it fails to predict the shift upwards in these dips which is shown in the numerical results. This is presumably a higher-order effect.

Again, the dips in the coherence can be attributed to the poles of B_{22} and the zeroes of A_{22}; in fact they are explained by the former here as seen from (44).

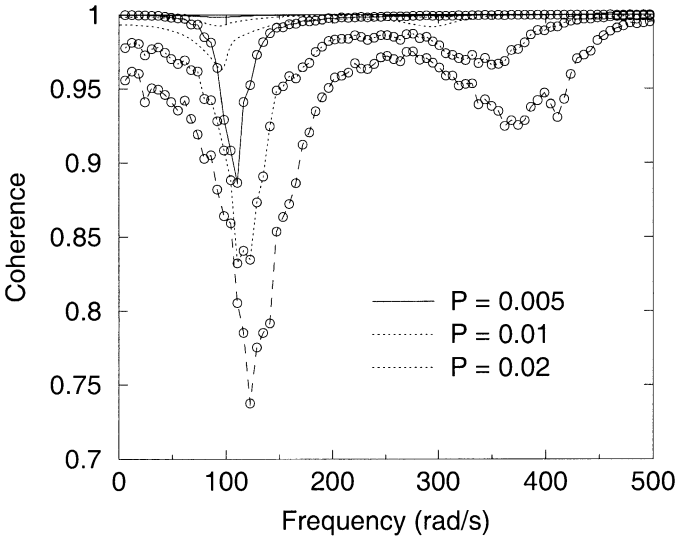

Fig. 5. Coherence from (2,2) Padé approximation for symmetrical ($k_2 = 0$) Duffing oscillator: $P = 0.005$ (solid line), $P = 0.01$ (dotted), $P = 0.02$ (dashed). Comparison with numerical simulation (lines with circles).

6. Discussion and conclusions

This paper extends the set of structural dynamic observables which can be approximated using the Volterra functional series. These approximations are valuable because they can give information about the pole structures of the various quantities which may later be exploited for identification purposes. The particular observable approximated here is the coherence function for the sdof asymmetric and symmetric Duffing oscillators. In the asymmetric case ($k_2 \neq 0$), the (1,1) approximation is obtained and shown to give excellent quantitative agreement with the results of numerical simulation. Specifically, the approximation shows dips in the coherence at low frequencies and at twice the linear natural frequency. At higher levels of excitation, there is also distortion evident at the natural frequency itself. What the approximation fails to capture is a dip at the third harmonic of the natural frequency when the level of excitation takes its higher values. This is consistent with the order of truncation of the approximation. The level of qualitative agreement is also fair with the 'true' distortions being factors of two or three greater than the rational approximation. Again, this is consistent with the effects of truncation. For the symmetric oscillator, the qualitative agreement is also good with the approximate coherence dipping at the natural frequency and third harmonic. However, in this case the qualitative agreement is less good with the numerical results showing relatively much greater dips than in the asymmetric case. Another effect not captured by the (2,2) approximation is the frequency shift upwards in the coherence dips for the numerical results. Again this appears to be a truncation effect and is reduced for the lower values of excitation level as one might expect.

These results were obtained in the belief that there is insight to be gained from the analytical approximations. There is also the possibility that appropriately accurate approximations may be used to extract information from measured data. This possibility lies somewhat in the future and

will require some means of extracting higher-order approximations. The authors are pursuing this with the aim of converting the calculations here from hand calculations with the assistance of computer algebra to full computer algebraic calculations.

Appendix A. Relations between cross-spectra

Two useful relationships between cross-spectra will be proved here. Although they could probably be derived faster using the machinery developed in Ref. [9], it is instructive to derive them from first principles, this also saves explaining the notation and techniques from Ref. [9].

Lemma. *Suppose the sequence* $y_i(t), i = 1, \ldots, \infty$ *is the Volterra expansion for a nonlinear system and that the excitation* $x(t)$ *is a white noise sequence with auto-correlation function* $\phi_{xx}(\tau) = P\delta(\tau)$ *then if* n *is odd,*

$$S_{y_1 x}(\omega) S_{x y_n}(\omega) = P S_{y_1 y_n}(\omega). \tag{A.1}$$

Proof. First, consider the term $S_{y_1 x}(\omega) S_{x y_n}(\omega)$.

Taking the inverse Fourier transform (with time variable τ)gives

$$\mathscr{F}^{-1}[S_{y_1 x}(\omega) S_{x y_n}(\omega)] = \phi_{y_1 x}(\tau) * \phi_{x y_n}(\tau) = \int_{-\infty}^{\infty} \mathrm{d}\tau'\, \phi_{y_1 x}(\tau') \phi_{x y_n}(\tau - \tau') \tag{A.2}$$

$$= \int_{-\infty}^{\infty} \mathrm{d}\tau'\, E[y_1(t) x(t + \tau')] E[x(t') y_n(t' + \tau - \tau')]$$

$$= \int_{-\infty}^{\infty} \mathrm{d}\tau'\, E[y_1(t) x(t + \tau')] E[y_n(t') x(t' - \tau + \tau')] \tag{A.3}$$

after using stationarity of the signals.

Substituting for the Volterra operators gives

$$\int_{-\infty}^{\infty} \mathrm{d}\tau'\, E\left[\int_{-\infty}^{\infty} \mathrm{d}\tau_1\, h_1(\tau_1) x(t - \tau_1) x(t + \tau') \right]$$
$$\times E\left[\int_{-\infty}^{\infty} \cdots \int_{-\infty}^{\infty} \mathrm{d}\eta_1 \ldots \mathrm{d}\eta_n\, h_n(\eta_1, \ldots, \eta_n) x(t' - \eta_1) \ldots x(t' - \eta_n) x(t' + \tau' - \tau) \right]. \tag{A.4}$$

Combining the terms and using the well-known decomposition of the expectation of a product of Gaussians into pair-wise expectations [4] gives

$$m_{1n} \int_{-\infty}^{\infty} \mathrm{d}\tau' \int_{-\infty}^{\infty} \mathrm{d}\tau_1\, h_1(\tau_1) \int_{-\infty}^{\infty} \cdots \int_{-\infty}^{\infty} \mathrm{d}\eta_1 \ldots \mathrm{d}\eta_n\, h_n(\eta_1, \ldots, \eta_n)$$
$$\times E[x(t - \tau_1) x(t + \tau)] E[x(t' - \eta_1) x(t' - \eta_2)] \cdots$$
$$E[x(t' - \eta_{n-2}) x(t' - \eta_{n-1})] E[x(t' - \eta_n) x(t' + \tau' - \tau)], \tag{A.5}$$

where the term m_{1n} counts the number of allowed permutations of the expectations. There is only one way to form the first expectation and there are clearly n ways to form the last. The case

of the intermediate $(n-1)/2$ terms is more complicated, but a little thought shows that there are $(n-1)!/(2^{(n-1)/2}((n-1)/2)!)$ ways of arranging them. The end result is

$$m_{1n} = \frac{n!}{2^{\frac{n-1}{2}}\left(\frac{n-1}{2}\right)!}. \tag{A.6}$$

Note that (A.5) depends critically on the symmetry of h_n under the interchange of any two symbols. The pair-wise expectations in (A.5) are simply autocorrelation functions of the input, so the integral becomes

$$\begin{aligned} m_{1n} \int_{-\infty}^{\infty} \mathrm{d}\tau' \int_{-\infty}^{\infty} \mathrm{d}\tau_1\, h_1(\tau_1) \int_{-\infty}^{\infty} \cdots \int_{-\infty}^{\infty} \mathrm{d}\eta_1 \ldots \mathrm{d}\eta_n\, h_n(\eta_1, \ldots, \eta_n) \\ \times \phi_{xx}(\tau' + \tau_1)\phi_{xx}(\eta_1 - \eta_2) \cdots \phi_{xx}(\eta_{n-2} - \eta_{n-1})\phi_{xx}(\eta_n + \tau' - \tau). \end{aligned} \tag{A.7}$$

But Gaussian inputs have been assumed with $\phi_{xx}(\tau) = P\delta(\tau)$, so the expression reduces to

$$\begin{aligned} m_{1n} P^{\frac{n+3}{2}} \int_{-\infty}^{\infty} \mathrm{d}\tau' \int_{-\infty}^{\infty} \mathrm{d}\tau_1\, h_1(\tau_1) \int_{-\infty}^{\infty} \cdots \int_{-\infty}^{\infty} \mathrm{d}\eta_1 \ldots \mathrm{d}\eta_n\, h_n(\eta_1, \ldots, \eta_n) \\ \times \delta(\tau' + \tau_1)\delta(\eta_1 - \eta_2) \ldots \delta(\eta_{n-2} - \eta_{n-1})\delta(\eta_n + \tau' - \tau). \end{aligned} \tag{A.8}$$

Arbitrarily choosing to project out the η variables with even indices yields

$$m_{1n} P^{\frac{n+3}{2}} \int_{-\infty}^{\infty} \mathrm{d}\tau' \int_{-\infty}^{\infty} \cdots \int_{-\infty}^{\infty} \overline{\mathrm{d}\eta_1 \ldots \mathrm{d}\eta_{n-2}}\, h_1(-\tau') h_n(\eta_1, \eta_1, \ldots \eta_{n-2}, \eta_{n-2}, \tau - \tau'), \tag{A.9}$$

where the overline indicates that only ηs with odd indices are included in the product.

Finally, changing $\tau' \longrightarrow -\tau'$ gives

$$\begin{aligned} &\mathscr{F}^{-1}[S_{y_1 x}(\omega) S_{x y_n}(\omega)] \\ &\quad = m_{1n} P^{\frac{n+3}{2}} \int_{-\infty}^{\infty} \mathrm{d}\tau' \int_{-\infty}^{\infty} \cdots \int_{-\infty}^{\infty} \overline{\mathrm{d}\eta_1 \ldots \mathrm{d}\eta_{n-2}}\, h_1(\tau') h_n(\eta_1, \eta_1, \ldots \eta_{n-2}, \eta_{n-2}, \tau + \tau'). \end{aligned} \tag{A.10}$$

Now, consider,

$$\mathscr{F}^{-1}[S_{y_1 y_n}(\omega) S_{xx}(\omega)] = P\mathscr{F}^{-1}[S_{y_1 y_n}(\omega)] = P\phi_{y_1 y_n}(\tau). \tag{A.11}$$

Considered as an expectation, this is simply

$$E[y_1(t - \tau) y_n(t)] \tag{A.12}$$

and in terms of Volterra kernels this is

$$\begin{aligned} E\Bigg[\int_{-\infty}^{\infty} \mathrm{d}\tau_1\, h_1(\tau_1) x(t - \tau - \tau_1) \\ \times \int_{-\infty}^{\infty} \cdots \int_{-\infty}^{\infty} \mathrm{d}\eta_1 \ldots \mathrm{d}\eta_n\, h_n(\eta_1, \ldots, \eta_n) x(t - \eta_1) \ldots x(t - \eta_n) \Bigg]. \end{aligned} \tag{A.13}$$

As before this is decomposed into pair-wise expectations,

$$\begin{aligned} m_{1n} \int_{-\infty}^{\infty} \mathrm{d}\tau_1\, h_1(\tau_1) \int_{-\infty}^{\infty} \cdots \int_{-\infty}^{\infty} \mathrm{d}\eta_1 \ldots \mathrm{d}\eta_n\, h_n(\eta_1, \ldots, \eta_n) \\ \times E[x(t - \tau' - \tau_1)x(t - \eta_1)] E[x(t - \eta_2)x(t - \eta_3)] \cdots E[x(t - \eta_{n-1})x(t - \eta_n)] \end{aligned} \tag{A.14}$$

and this is

$$m_{1n}\int_{-\infty}^{\infty}\mathrm{d}\tau_1\, h_1(\tau_1)\int_{-\infty}^{\infty}\ldots\int_{-\infty}^{\infty}\mathrm{d}\eta_1\ldots\mathrm{d}\eta_n\, h_n(\eta_1,\ldots,\eta_n)$$
$$\times\phi_{xx}(\tau_1+\tau'-\eta_1)\phi_{xx}(\eta_2-\eta_3)\ldots\phi_{xx}(\eta_{n-1}-\eta_n) \tag{A.15}$$

but because x is white-Gaussian, this is

$$m_{1n}P^{(n+3)/2}\int_{-\infty}^{\infty}\mathrm{d}\tau_1\, h_1(\tau_1)\int_{-\infty}^{\infty}\ldots\int_{-\infty}^{\infty}\mathrm{d}\eta_1\ldots\mathrm{d}\eta_n\, h_n(\eta_1,\ldots,\eta_n)$$
$$\times\delta(\tau_1+\tau'-\eta_1)\delta(\eta_2-\eta_3)\ldots\delta(\eta_{n-1}-\eta_n). \tag{A.16}$$

Projecting out the odd variables using the delta functions leads to the expression,

$$m_{1n}P^{(n+3)/2}\int_{-\infty}^{\infty}\mathrm{d}\tau_1\int_{-\infty}^{\infty}\ldots\int_{-\infty}^{\infty}\overline{\mathrm{d}\eta_2\ldots\mathrm{d}\eta_{n-1}}h_1(\tau_1)h_n(\tau_1+\tau,\eta_2,\eta_2,\ldots\eta_{n-1},\eta_{n-1}), \tag{A.17}$$

where the overline omits the odd indexed variables now.

Using the symmetry properties of h_n under any permutations of indices and making a trivial relabelling of the integration variables leads to the same expression as in (A.10) and this establishes that

$$\mathscr{F}^{-1}[S_{y_1x}(\omega)S_{xy_n}(\omega)] = P\phi_{y_1y_n}(\tau) \tag{A.18}$$

so that taking the Fourier transform establishes the desired result. The relation can obviously also be proved by computing $S_{y_1y_n}$ and showing that it factorises into terms of the form (A.1).

The next result of use is:

Lemma. *Under the same conditions as the previous lemma,*

$$PS_{y_3y_n}(\omega) = S_{y_3x}(\omega)S_{xy_n}(\omega) + \frac{q_{3n}P^{\frac{n+5}{2}}}{(2\pi)^{\frac{n+1}{2}}}\int_{-\infty}^{\infty}\int_{-\infty}^{\infty}\mathrm{d}\omega_1\mathrm{d}\omega_2\int_{-\infty}^{\infty}\cdots\int_{-\infty}^{\infty}\overline{\mathrm{d}\eta_4\ldots\mathrm{d}\eta_{n-1}}$$
$$\times H_3(\omega_1,\omega_2,-\omega-\omega_1-\omega_2)H_3(-\omega_1,-\omega_2,\omega+\omega_1$$
$$+\omega_2,\eta_4,-\eta_4,\ldots,\eta_{n-1},-\eta_{n-1}). \tag{A.19}$$

Proof. First consider the term $S_{y_3x}(\omega)S_{xy_n}(\omega)$. The manipulations needed are very similar to those in the first lemma. First, take the inverse Fourier transform and convert to the correlation,

$$\mathscr{F}^{-1}[S_{y_3x}(\omega)S_{xy_n}(\omega)] = \int_{-\infty}^{\infty}\mathrm{d}\tau'\,\phi_{y_3x}(\tau')\phi_{xy_n}(\tau-\tau'). \tag{A.20}$$

After replacing the correlations by the appropriate expectations and substituting the Volterra operators for y_3 and y_n, one obtains

$$\begin{aligned} m_{3n}\int_{-\infty}^{\infty}\mathrm{d}\tau'\int_{-\infty}^{\infty}\int_{-\infty}^{\infty}\int_{-\infty}^{\infty}\mathrm{d}\tau_1\,\mathrm{d}\tau_2\,\mathrm{d}\tau_2\int_{-\infty}^{\infty}\cdots\int_{-\infty}^{\infty}\mathrm{d}\eta_1\ldots\mathrm{d}\eta_n\,h_2(\tau_1,\tau_2,\tau_3)h_n(\eta_1,\ldots,\eta_n)\\ \times E[x(t-\tau_1)x(t-\tau_2)]E[x(t-\tau_3)x(t+\tau')]\\ \times E[x(t'-\eta_1)x(t'-\eta_2)]\ldots E[x(t'-\eta_{n-2})x(t'-\eta_{n-1})]\\ \times E[x(t'-\eta_n)x(t'-\tau+\tau')], \end{aligned} \tag{A.21}$$

where the number of ways of combining the arguments of the expectations is

$$m_{3n}=\frac{3n!}{2^{\left(\frac{n-1}{2}\right)}\left(\frac{n-1}{2}\right)!}. \tag{A.22}$$

Substituting the correlation function for Gaussian noise, gives the final result,

$$\begin{aligned} m_{3n}P^{(5+n)/2}\int_{-\infty}^{\infty}\int_{-\infty}^{\infty}\mathrm{d}\tau_1\,\mathrm{d}\tau_3\int_{-\infty}^{\infty}\cdots\int_{-\infty}^{\infty}\overline{\mathrm{d}\eta_1\ldots\mathrm{d}\eta_{n-2}}\,h(\tau_1,\tau_1,\tau_3)\\ \times h(\eta_1,\eta_1,\ldots,\eta_{n-2},\eta_{n-2},\tau+\tau_3). \end{aligned} \tag{A.23}$$

Next consider,

$$\mathscr{F}^{-1}[S_{y_3y_n}(\omega)S_{xx}(\omega)]=\int_{-\infty}^{\infty}\mathrm{d}\tau'\,\phi_{y_3y_n}(\tau')\phi_{xx}(\tau-\tau'). \tag{A.24}$$

After substituting for the ϕs and introducing the Volterra operators, the resulting integral contains the product of expectations,

$$\begin{aligned} E[x(t-\tau_1)\ldots x(t-\tau_3)x(t+\tau'-\eta_1)\ldots x(t+\tau-\eta_n)]\\ \times E[x(t')x(t'+\tau+\tau')] \end{aligned} \tag{A.25}$$

This leads to two distinct pairwise products of expectations. In the first, the τ variables are grouped together thus, $E[x(t-\tau_1)x(t-\tau_2)]E[x(t-\tau_3)x(t+\tau'-\eta_i)]\ldots$ and this leads eventually to an integral identical to (A.23). In the second grouping, the τ variables are all paired up with η variables leading to $E[x(t-\tau_1)x(t+\tau'-\eta_i)]E[x(t-\tau_2)x(t+\tau'-\eta_j)]E[x(t-\tau_3)x(t+\tau'-\eta_k)]\ldots$ This leads to a final integral,

$$\begin{aligned} I_{3n}=q_{3n}\int_{-\infty}^{\infty}\cdots\int_{-\infty}^{\infty}\mathrm{d}\eta_1\,\mathrm{d}\eta_2\,\mathrm{d}\eta_3\,\overline{\mathrm{d}\eta_4\ldots\mathrm{d}\eta_{n-1}}\\ \times h_3(\eta_1-\tau,\eta_2-\tau,\eta_3-\tau)h_n(\eta_1,\eta_2,\eta_3,\eta_4,\eta_4,\ldots,\eta_{n-1}\eta_{n-1}), \end{aligned} \tag{A.26}$$

where

$$q_{3n} = \frac{6(n-3)!}{2^{((n-3)/2)}(\frac{n-3}{2})!}. \tag{A.27}$$

Now taking the Fourier transform of the integrals obtained so far gives

$$S_{y_3x}(\omega)S_{xy_n}(\omega) = PS_{y_3y_n}(\omega) + \mathscr{F}[I_{3n}] \tag{A.28}$$

and in order to establish the required result, one has simply to evaluate the Fourier transform of (A.26).

First, take the multidimensional FT of (A.26) and replace each of the h_j with their FT (see Eq. (A.3) in the main body of the paper).

$$\begin{aligned}
&\mathscr{F}[I_{3n}]\\
&= q_{3n}P^{(5+n)/2}\int_{-\infty}^{\infty} \mathrm{d}\tau\, \mathrm{e}^{-\mathrm{i}\omega\tau}\int_{-\infty}^{\infty}\int_{-\infty}^{\infty}\int_{-\infty}^{\infty} \mathrm{d}\eta_1\, \mathrm{d}\eta_2\, \mathrm{d}\eta_3 \int_{-\infty}^{\infty}\cdots\int_{-\infty}^{\infty} \overline{\mathrm{d}\eta_4 \ldots \mathrm{d}\eta_{n-1}}\\
&\quad\times \frac{1}{(2\pi)^3}\int_{-\infty}^{\infty}\int_{-\infty}^{\infty}\int_{-\infty}^{\infty} \mathrm{d}\omega_1\, \mathrm{d}\omega_2\, \mathrm{d}\omega_3 H_3(\omega_1,\omega_2,\omega_3)\mathrm{e}^{\mathrm{i}[\omega_1(\eta_1-\tau)+\omega_2(\eta_2-\tau)+\omega_3(\eta_3-\tau)]}\\
&\quad\times \frac{1}{(2\pi)^n}\int_{-\infty}^{\infty}\cdots\int_{-\infty}^{\infty} \mathrm{d}\alpha_1 \ldots \mathrm{d}\alpha_n\, H_n(\alpha_1,\ldots,\alpha_n)\mathrm{e}^{\mathrm{i}[\alpha_1\eta_1+\alpha_2\eta_2+\alpha_3\eta_3+(\alpha_4+\alpha_5)\eta_4+\cdots+(\alpha_{n-1}+\alpha_n)\eta_n]}.
\end{aligned} \tag{A.29}$$

First, one integrates out the variables η_4 to η_{n-1}. This is accomplished by collecting the factors

$$\frac{1}{2\pi}\int_{-\infty}^{\infty} \mathrm{d}\eta_i \mathrm{e}^{\mathrm{i}(\alpha_i+\alpha_{i+1})\eta_i} = \delta(\alpha_i+\alpha_{i+1}). \tag{A.30}$$

and using the projection property of the delta functions. This gives

$$\begin{aligned}
&q_{3n}\frac{P^{\frac{5+n}{2}}}{(2\pi)^{\frac{n+3}{2}}}\int_{-\infty}^{\infty}\cdots\int_{-\infty}^{\infty} \mathrm{d}\tau\, \mathrm{d}\omega_1\, \mathrm{d}\omega_2\, \mathrm{d}\omega_3\, \mathrm{d}\alpha_1\, \mathrm{d}\alpha_2\, \mathrm{d}\alpha_3 \overline{\mathrm{d}\alpha_4 \ldots \mathrm{d}\alpha_{n-1}}\\
&\quad\times H_3(\omega_1,\omega_2,\omega_3)H_n(\alpha_1,\alpha_2,\alpha_3,\alpha_4,-\alpha_4,\ldots,\alpha_{n-1},-\alpha_{n-1})\\
&\quad\times\left\{\frac{1}{2\pi}\int_{-\infty}^{\infty} \mathrm{d}\eta_1\, \mathrm{e}^{\mathrm{i}\eta_1(\omega_1+\alpha_1)}\right\}\left\{\frac{1}{2\pi}\int_{-\infty}^{\infty} \mathrm{d}\eta_2\, \mathrm{e}^{\mathrm{i}\eta_2(\omega_2+\alpha_2)}\right\}\\
&\quad\times\left\{\frac{1}{2\pi}\int_{-\infty}^{\infty} \mathrm{d}\eta_3\, \mathrm{e}^{\mathrm{i}\eta_3(\omega_3+\alpha_3)}\right\}\mathrm{e}^{-\mathrm{i}\tau(\omega+\omega_1+\omega_2+\omega_3)}
\end{aligned} \tag{A.31}$$

after a little rearrangement. Now, the bracketed quantities in the last equation are delta functions $\delta(\omega_i + \alpha_i)$ and can be used to project out the first three αs, yielding

$$q_{3n}\frac{P^{(5+n)/2}}{(2\pi)^{(n+3)/2}}\int_{-\infty}^{\infty}\cdots\int_{-\infty}^{\infty}\mathrm{d}\omega_1\,\mathrm{d}\omega_2\,\mathrm{d}\omega_3\,\overline{\mathrm{d}\alpha_4\ldots\mathrm{d}\alpha_{n-1}}$$
$$\times H_3(\omega_1,\omega_2,\omega_3)H_n(-\omega_1,-\omega_2,-\omega_3,\alpha_4,-\alpha_4,\ldots,\alpha_{n-1},-\alpha_{n-1})$$
$$\times\left\{\frac{1}{2\pi}\int_{-\infty}^{\infty}\mathrm{d}\tau\,\mathrm{e}^{\mathrm{i}\tau(\omega+\omega_1+\omega_2+\omega_3)}\right\} \tag{A.32}$$

and the bracketed quantity is again a delta function $\delta(\omega+\omega_1+\omega_2+\omega_2)$. If this is used to project out τ, the required result follows.

A specific result used in the main body of this paper is obtained by setting $n=3$ in the lemma. This gives

$$PS_{y_3y_3} = |S_{y_3x}|^2 + \frac{6P^4}{(2\pi)^2}\int_{-\infty}^{\infty}\int_{-\infty}^{\infty}\mathrm{d}\omega_1\,\mathrm{d}\omega_2|H_3(\omega_1,\omega_1,-\omega-\omega_1-\omega_2)|^2 \tag{A.33}$$

and from this it follows that:

$$PS_{y_3y_3} > |S_{y_3x}|^2. \tag{A.34}$$

References

[1] K. Worden, G. Manson, Random vibrations of a Duffing oscillator using the Volterra series, *Journal of Sound and Vibration* 217 (1998) 781–789.

[2] K. Worden, G. Manson, Random vibrations of a multi degree-of-freedom nonlinear system using the Volterra series, *Journal of Sound and Vibration* 226 (1999) 397–405.

[3] V. Volterra, *Theory of Functionals and Integral Equations*, Dover Publications, New York, 1959.

[4] M. Schetzen, *The Volterra and Wiener Theories of Nonlinear Systems*, Wiley Interscience Publication, New York, 1980.

[5] M.F. Dimentberg, *Statistical Dynamics of Nonlinear and Time-Varying Systems*, Research Studies Press, Taunton, 1988.

[6] K. Worden, G.R. Tomlinson, *Nonlinearity in Structural Dynamics*, Institute of Physics, 2001.

[7] J.S. Bendat, A.G. Piersol, *Random Data—Analysis and Measurement Procedures*, second ed., Wiley Interscience, New York, 1986.

[8] M.I. Friswell, J.E.T. Penny, Crack modelling for structural health monitoring, *International Journal of Structural Health Monitoring*, 2002.

[9] E. Bedrosian, S.O. Rice, The output properties of Volterra systems driven by harmonic and Gaussian inputs, *Proceedings of IEEE* 59 (1971) 1688–1707.